Received: 4 September 2023 | Accepted: 19 January 2024

DOI: 10.1002/cai2.127

ORIGINAL ARTICLE

CANCER INNOVATION

High-fat-diet-induced obesity promotes simultaneous progression of lung cancer and atherosclerosis in apolipoprotein E-knockout mice

Yihao Wang[1] | **Kaixin Yan**[1] | **Han Duan**[2] | **Ning Tao**[2] | **Shaoning Zhu**[1] | **Yuning Zhang**[2] | **Yonggang You**[3] | **Zhen Zhang**[3] | **Hua Wang**[2] | **Shunying Hu**[1]

[1]Department of Cardiology, Chinese PLA General Hospital, Beijing, China

[2]Beijing Institute of Radiation Medicine, Beijing, China

[3]Department of Orthopaedics, Chinese PLA General Hospital, Beijing, China

Correspondence

Shunying Hu, Department of Cardiology, Chinese PLA General Hospital, 28 Fuxing Rd, Beijing 100853, China.
Email: hsylily@163.com

Hua Wang, Beijing Institute of Radiation Medicine, 27 Taiping Rd, Beijing 100850, China.
Email: 18511712135@163.com

Funding information

National Natural Science Foundation of China, Grant/Award Numbers: 81770237, 82173450

Abstract

Background: Clinical studies have shown that atherosclerotic cardiovascular disease and cancer often co-exist in the same individual. The present study aimed to investigate the role of high-fat-diet (HFD)-induced obesity in the coexistence of the two diseases and the underlying mechanism in apolipoprotein E-knockout ($ApoE^{-/-}$) mice.

Methods: Male $ApoE^{-/-}$ mice were fed with a HFD or a normal diet (ND) for 15 weeks. On the first day of Week 13, the mice were inoculated subcutaneously in the right axilla with Lewis lung cancer cells. At Weeks 12 and 15, serum lectin-like oxidized low-density lipoprotein receptor-1 (LOX-1) and vascular endothelial growth factor levels were measured by enzyme-linked immunosorbent assay, and blood monocytes and macrophages were measured by fluorescence-activated cell sorting. At Week 15, the volume and weight of the local subcutaneous lung cancer and metastatic lung cancer and the amount of aortic atherosclerosis were measured.

Results: At Week 15, compared with mice in the ND group, those in the HFD group had a larger volume of local subcutaneous cancer ($p = 0.0004$), heavier tumors ($p = 0.0235$), more metastatic cancer in the lungs ($p < 0.0001$), a larger area of lung involved in metastatic cancer ($p = 0.0031$), and larger areas of atherosclerosis in the aorta ($p < 0.0001$). At Week 12, serum LOX-1, serum vascular endothelial growth factor, and proportions of blood monocytes and macrophages were significantly higher in the HFD group than those in the ND group ($p = 0.0002$, $p = 0.0029$, $p = 0.0480$, and $p = 0.0106$, respectively);

Abbreviations: $ApoE^{-/-}$, apolipoprotein E-knockout; ASCVD, atherosclerotic cardiovascular disease; HDL-C, high-density lipoprotein cholesterol; HFD, high-fat diet; LDL-C, low-density lipoprotein cholesterol; LLC, Lewis lung cancer; LOX-1, lectin-like oxidized low-density lipoprotein receptor-1; ND, normal diet; TC, total cholesterol; VEGF, vascular endothelial growth factor.

Yihao Wang and Kaixin Yan contributed equally to this study and shared the first authorship.

this trend persisted until Week 15 ($p = 0.0014$, $p = 0.0012$, $p = 0.0001$, and $p = 0.0204$).

Conclusions: In this study, HFD-induced obesity could simultaneously promote progression of lung cancer and atherosclerosis in the same mouse. HFD-induced upregulation of LOX-1 may play an important role in the simultaneous progression of these two conditions via the inflammatory response and VEGF.

KEYWORDS

atherosclerosis, high-fat diet, LOX-1, lung cancer, obesity

1 | INTRODUCTION

Atherosclerotic cardiovascular disease (ASCVD) and cancer are two chronic diseases that are known to be the leading causes of death worldwide [1]. Atherosclerosis is the most common condition underlying cardiovascular disease [2, 3], which has a multifactorial etiology. The most common risk factors are hypercholesterolemia, hypertension, diabetes mellitus, cigarette smoking, age, male sex, and a strong family history. A sedentary lifestyle, obesity, a diet high in saturated and transfatty acids, and certain genetic mutations also contribute to the risk of cardiovascular disease [4].

Although cancer is widely considered to be different from atherosclerosis in terms of its clinical manifestations and pathogenesis, there is an increasing body of evidence showing coexistence of atherosclerosis and cancer in the same individuals [5]. A cohort study that investigated the incidence of new cancers in 32,095 patients with cardiovascular disease according to the presence or absence of atherosclerosis found that the incidence of new tumors was twice as high in patients with ASCVD [6].

One possible reason for the coexistence of atherosclerosis and cancer in the same individuals is the similarity between the risk factors for the two conditions, such as age, sedentary lifestyle, smoking, and a diet rich in fat and carbohydrates [7]. Obesity and hyperlipidemia are well-known risk factors for atherosclerosis and have been demonstrated to have a significant impact on tumorigenesis and the invasiveness of cancer in murine models and in vitro research [8–10]. Until now, no study has investigated whether high-fat-diet (HFD)-induced obesity can simultaneously promote progression of atherosclerosis and cancer in the same individual.

Clinical research by our group has demonstrated an association between the anatomical severity of coronary artery disease and the risk of lung cancer [11, 12]; however, the underlying mechanism remains elusive. In the present study, we investigated the impact of HFD-induced obesity on progression of both lung cancer and atherosclerosis in the same mice. Lectin-like oxidized low-density lipoprotein receptor-1 (LOX-1) is becoming an important target in terms of the link between atherosclerosis and cancer [13, 14]. We observed an effect of HFD on the serum LOX-1 level in this study. The circulating vascular endothelial growth factor (VEGF) level was also assessed to elucidate the role of LOX-1 in the coexistence of atherosclerosis and lung cancer. We detected changes in levels of monocytes and macrophages, which have an important role in the pathogenesis of both atherosclerosis and cancer [15, 16].

2 | MATERIALS AND METHODS

2.1 | Animals and protocols

Six-week-old male apolipoprotein E-knockout ($ApoE^{-/-}$) mice with a C57BL/6J background were purchased from Beijing Vital River Laboratory Animal Technology Co., Ltd. All animals were kept in a specific pathogen-free animal facility on a 12/12-h light/dark cycle at (22 ± 2)°C and 50% relative humidity. Five mice were housed per cage. The mice were randomly allocated to receive a normal diet (the ND group, $n = 14$) or a HFD (77.75% basal diet + 21% lard +1.25% cholesterol; the HFD group, $n = 14$) for 15 weeks. The mice were subcutaneously inoculated with Lewis lung cancer (LLC) cells at the first day of Week 13. Thereafter, the mice were monitored continuously for the development of lung cancer. After 15 weeks (Day 105), cervical dislocation euthanized mice, and the aorta and lungs were removed for evaluation of atherosclerosis in the aorta and metastasis of lung cancer, respectively. Body length, body weight, and abdominal circumference were measured at Weeks 0, 4, 8, and 12. No adverse events were observed during any of the study procedures.

2.2 | Lipid profile

At Week 12, the lipid profile was determined in venous blood collected from the inner canthus vein, from which the serum was separated for measurement of blood lipid levels. Lipids included total cholesterol (TC), triglycerides, high-density lipoprotein cholesterol (HDL-C), and low-density lipoprotein cholesterol (LDL-C), which were measured using an automated biochemistry instrument following the manufacturer's protocol (Servicebio Technology).

2.3 | Culture of LLC cells

The LLC cells were purchased from Beijing Baiaosicheng Biotechnology Co., Ltd. and cultured in Dulbecco's modified Eagle medium (Gibco) supplemented with 10% fetal calf serum in a humidified atmosphere with 5% CO_2 at 37°C.

2.4 | Tumor allograft model

At Week 13 (Day 85), 1×10^6 LLC cells in 100 μL of phosphate-buffered saline (PBS) were inoculated subcutaneously in the right axilla of each mouse to construct an allograft tumor model. After inoculation with LLC cells, the mice were fed with ND or HFD for a further 3 weeks.

2.5 | Measurement of tumor volume and weight

The local subcutaneous cancers could be seen from Week 14 (Day 11 postinoculation of LLC cells) onward. The longest and shortest diameters of the tumors were measured using vernier calipers at Day 11, 14, 17, and 21 postinoculations with LLC cells. The tumor volume was calculatedhas length × width^2/2. On Day 21, the local subcutaneous tumors were removed and weighed.

2.6 | Measurement of metastatic lung cancer

The mice were euthanized on Day 21 postinoculation. The lungs were harvested for evaluation of metastasis of lung cancer. The number of metastatic tumors on the lung surface was calculated visually. Hematoxylin–eosin staining was performed after fixation of the lungs with 4% paraformaldehyde to observe the metastasis of lung cancer in the maximum cross-sectional area of the lung. The area of lung involved in metastatic cancer were measured using CaseViewer software (3DHISTECH).

2.7 | Assessment of atherosclerosis

At Day 21 post-LLC transplantation, the mice were euthanized, and the vasculature in the heart was perfused with 10 mL of PBS followed by 5 mL of buffered formalin (Thermo Fisher Scientific). The entire length of the aorta, from the heart, including the subclavian and right and left carotid arteries, through to 2–5 mm after bifurcation of the iliac artery, was dissected free of fat and postfixed in buffered formalin for 24 h at 4°C and then stored in PBS at 4°C. The aorta was stained with oil red-O, which identifies neutral lipids in plaque, to quantify the lesion burden. After staining, the aorta was opened, laid flat, and digitally scanned [17]. Morphometric measurements of the aorta were obtained in a blinded fashion. Three independent measurements of lesion area (red pixels) were selected and averaged for each aorta using Adobe Photoshop software (Adobe Inc.). Similarly, the total area of the aorta was determined. The lesion area was expressed as the mean percentage ± standard deviation of total aortic area.

2.8 | Measurement of serum LOX-1 and VEGF

Serum LOX-1 and VEGF levels were measured by enzyme-linked immunosorbent assay following the protocol outlined by the manufacturer (Delos Biotechnology Co.).

2.9 | Flow cytometry analysis of blood monocytes and macrophages

Peripheral blood was collected from the medial canthal vein and anticoagulated using heparin sodium. After lysing the red blood cells in the peripheral blood sample, it was incubated with mF4/80-PE (macrophages), mCD11b APC, and mLY6C-FITC (monocytes) (BD Pharmingen). After two washes, collect samples and analyze them using the FACS Calibur system (BD Biosciences) to measure the levels of monocytes and macrophages.

2.10 | Statistical analysis

The data are presented as the mean ± standard deviation. Means were compared between the two groups using the Student's *t* test. All statistical analyses were performed

using GraphPad Prism version 5 (GraphPad Software Inc.). All tests were two-tailed, and a p-value < 0.05 was considered statistically significant.

3 | RESULTS

3.1 | Body length, body weight, abdominal circumference, and lipid concentrations

The morphometric data for the mice after 12 weeks of a HFD are shown in Figure 1. Body length, body weight, and abdominal circumference were evaluated at 4-week intervals in both groups before inoculation with LLC cells. There was no significant difference in body length between the HFD group and the ND group ((7.750 ± 0.418) cm vs. (7.733 ± 0.501) cm at Week 12, $p = 0.9513$). At Week 12, weight gain was significantly greater in the HFD group than in the ND group ((33.860 ± 1.163) g vs. (31.870 ± 1.807) g, $p = 0.0464$), as was abdominal circumference ((9.650 ± 0.207) cm vs. (8.933 ± 0.427) cm at Week 1, $p = 0.0041$) (Figure 1a–c). The morphology of mice after 12 weeks of a HFD or a ND is shown in Figure 1d.

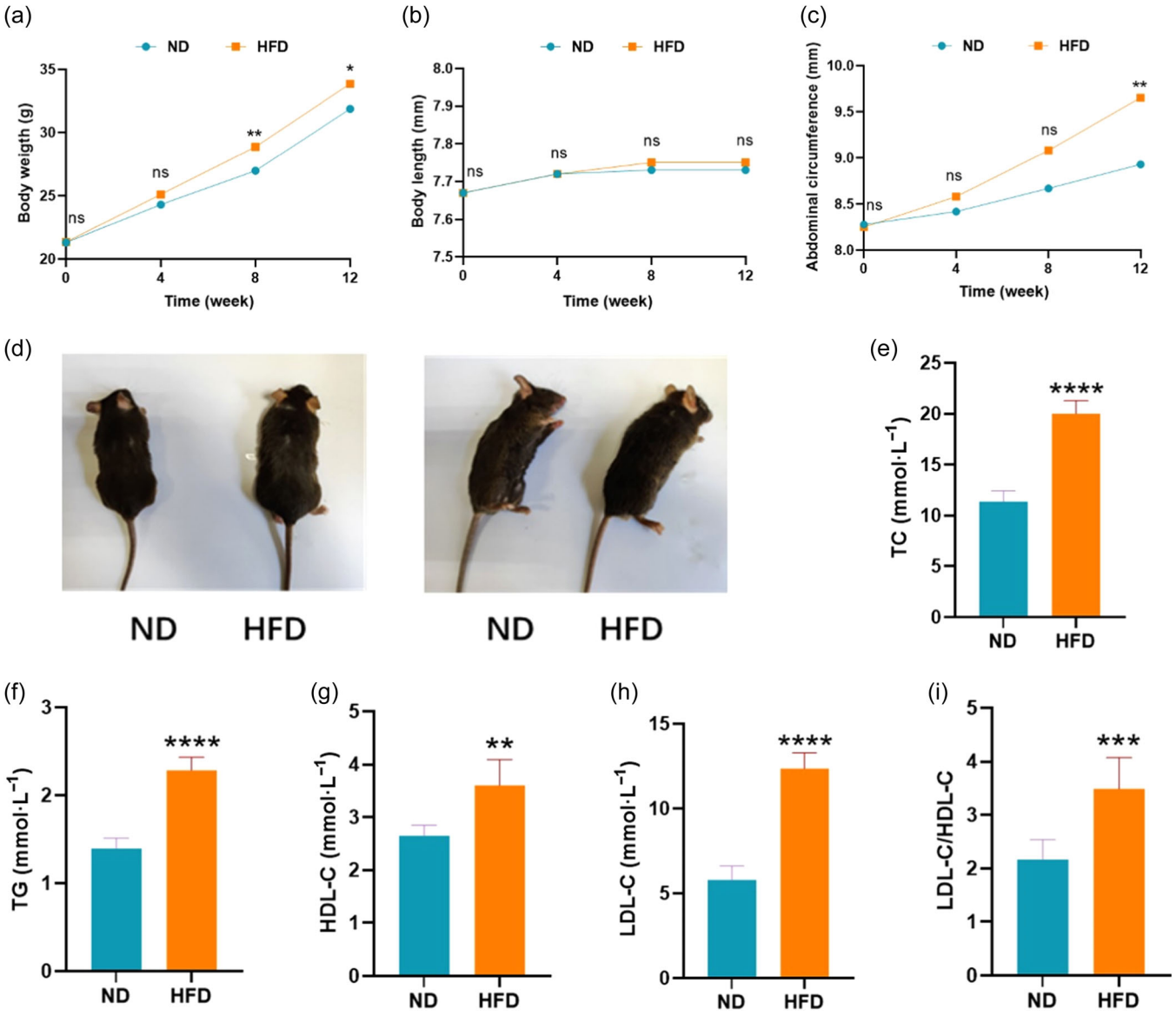

FIGURE 1 Morphometric changes and lipid concentrations in mice at 12 weeks. Changes in (a) body length, (b) body weight, and (c) abdominal circumference at Weeks 0, 4, 8, and 12. (d) Photographs showing top and profile views of the mice after 12 weeks of a high-fat diet or a normal diet. (e) TC, (f) TG, (g) HDL-C, (h) LDL-C, and (i) the LDL-C/HDL-C ratio at Week 12. The data are presented as the mean ± standard deviation ($n = 6$). *$p < 0.05$, **$p < 0.01$, ***$p < 0.001$, ****$p < 0.0001$ versus the ND group. HDL-C, high-density lipoprotein cholesterol; HFD, high-fat diet; LDL-C, low-density lipoprotein cholesterol; ND, normal diet; TC, total cholesterol; TG, triglycerides.

The lipid profile was assessed at Week 12 before inoculation with LLC cells. Mice in the HFD group had higher levels of TC ((20.020 ± 1.284) mmol/L vs. (11.360 ± 1.058) mmol/L, $p < 0.0001$), triglycerides ((2.287 ± 0.1456) mmol/L vs. (1.393 ± 0.1227) mmol/L, $p < 0.0001$), HDL-C ((3.604 ± 0.490) mmol/L vs. (2.653 ± 0.199) mmol/L, $p = 0.0013$), and LDL-C ((12.360 ± 0.926) mmol/L vs. (5.791 ± 0.820) mmol/L, $p < 0.0001$). The LDL-C/HDL-C ratio was higher in the HFD group than in the ND group (3.488 ± 0.585 vs. 2.163 ± 0.380, $p = 0.0009$) (Figure 1e–i).

3.2 | HFD promoted simultaneous progression of lung cancer and atherosclerosis

The subcutaneous tumors were visible to the eye from Day 11 postinoculation with LLC cells, and their volumes were measured on Days 11, 14, 17, and 21 postinoculations. Interestingly, the tumor volume was smaller in the HFD group than in the ND group at Day 11 ((21.19 ± 6.07) mm^3 vs. (25.25 ± 13.93) mm^3, $p = 0.1543$); however, the difference was not statistically significant. On Days 14, 17, and 21, the tumor volume was larger in the HFD group than in the ND group ((151.90 ± 42.25) mm^3 vs. (80.13 ± 36.95) mm^3, $p = 0.0088$; (457.50 ± 168.20) mm^3 vs. (269.50 ± 33.78) mm^3, $p = 0.0229$; and (1657.21 ± 167.70) mm^3 vs. (1132.10 ± 183.10) mm^3, $p = 0.0004$, respectively).

The tumors and lungs were harvested from the mice after they were euthanized on Day 21 postinoculation with LLC cells. Tumors were heavier in the HFD group than in the ND group ((1.972 ± 0.609) g vs. (1.205 ± 0.351) g, $p = 0.0235$) (Figure 2a,b). These results indicated that hyperlipidemia may delay onset of a tumor, but when a tumor is formed, the tumor volume increases rapidly, exceeding the normal growth rate of the tumor.

There were more metastatic tumors on the surface of the lungs in the HFD group than in the ND group (18.500 ± 3.674 vs. 8.010 ± 1.265, $p < 0.0001$). Hematoxylin–eosin staining of the maximum cross-sectional area of the lungs showed that the total area of the lung involved in metastatic disease was significantly greater in the HFD group than in the ND group ((5.983 ± 1.710) mm^2 vs. (2.967 ± 0.857) mm^2, $p = 0.0031$) (Figure 2c–f).

At Week 15, the aorta was removed for oil red-O staining. The results showed that the area of atherosclerosis was significantly larger in the HFD group than in the ND group (14.200% ± 2.347% vs. 1.868% ± 0.403%, $p < 0.0001$) (Figure 2g,h), indicating that a HFD increases the burden of atherosclerosis.

3.3 | HFD induced LOX-1 and VEGF expression

At 12 weeks (before inoculation of LLC) and at Week 15 (i.e., Day 21 postinoculation of LLC), blood was collected from the epicanthus vein of each mouse, and serum was harvested for measurement of serum LOX-1 and VEGF levels by enzyme-linked immunosorbent assay.

At Weeks 12 and 15, the serum LOX-1 level was higher in the HFD group than in the ND group ((32.032 ± 1.979) pg/mL vs. (22.453 ± 3.688) pg/mL, $p = 0.0002$ and (36.820 ± 1.805) pg/mL vs. (30.691 ± 2.921) pg/mL, $p = 0.0014$, respectively) (Figure 3a). The serum VEGF level was also significantly higher in the HFD group at Weeks 12 and 15 ((27.153 ± 4.960) pg/mL vs. (22.422 ± 4.140) pg/mL, $p = 0.0029$ and (30.663 ± 1.994) pg/mL vs. (25.350 ± 2.105) pg/mL, $p = 0.0012$, respectively) (Figure 3b).

3.4 | HFD increased the inflammatory response in blood

The proportion of monocytes and macrophages in the HFD group was higher than that in the ND group. The proportion of monocytes in the HFD group was higher than that in the ND group at Week 12 (31.623 ± 7.359 vs. 23.501 ± 4.876, $p = 0.0480$) and Week 15 (69.800 ± 7.148 vs. 37.680 ± 10.520, $p = 0.0001$) (Figure 4a,b). The proportion of macrophages in the HFD group is still higher at Week 12 (20.427 ± 5.207 vs. 13.253 ± 2.083, $p = 0.0106$) and Week 15 (16.232 ± 1.713 vs. 12.881 ± 2.441, $p = 0.0204$) (Figure 4c,d).

4 | DISCUSSION

To the best of our knowledge, this is the first basic study to investigate the effect of HFD-induced obesity on the progression of both lung cancer and atherosclerosis in the same mice. Our data show that an HFD simultaneously promoted the progression of lung cancer and aortic atherosclerosis in mice and also induced expression of LOX-1 and VEGF as well as increased proportions of monocytes and macrophages. Therefore, obesity could promote the simultaneous progression of lung cancer and atherosclerosis in the same individual possibly through a LOX-1-related pathway.

Both ASCVD and lung cancer are multifactorial diseases with a serious impact on human health. In the past, these two diseases were widely considered to be completely different in terms of their pathogenesis, clinical manifestations, and prognosis. However, in recent decades, an increasing body of evidence has

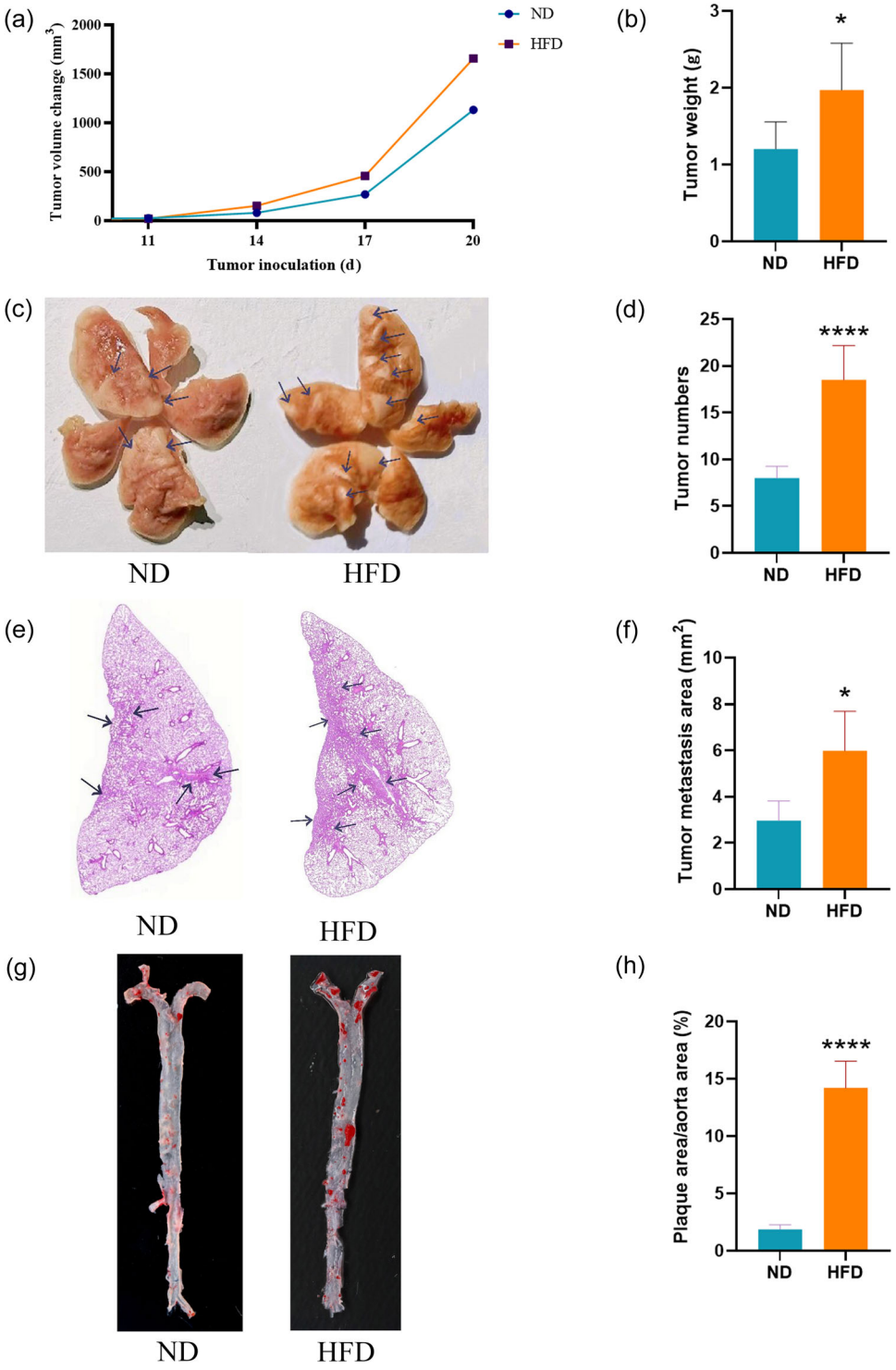

FIGURE 2 Progression of lung cancer and atherosclerosis in the ND and HFD groups at Week 15. (a) Lung cancer volume on Days 0, 11, 14, 17, and 21 after inoculation with LLC cells. (b) Lung cancer weight on Day 21 after inoculation with LLC cells. (c) Photograph showing lung nodules on Day 21 after inoculation with LLC cells (arrows indicate visible lung tumors). (d) Quantification analysis of the numbers of metastatic lung cancers on the lung surface in the two groups. (e) Representative HE staining of lung sections on Day 21 after inoculation with LLC cells (arrows indicate visible metastatic lung tumors). (f) Quantification analysis of the area of tumor metastasis in the lung with HE staining in the two groups. (g) Representative image of an aorta stained with oil red-O on Day 21 after inoculation with LLC cells. (h) Quantification analysis of oil red-O staining area in the aorta in the two groups. The data are shown as the mean ± standard deviation ($n = 6$). *$p < 0.05$, ****$p < 0.0001$ versus the ND group. HE, hematoxylin-eosin; HFD, high-fat diet; LLC, Lewis lung cancer; ND, normal diet.

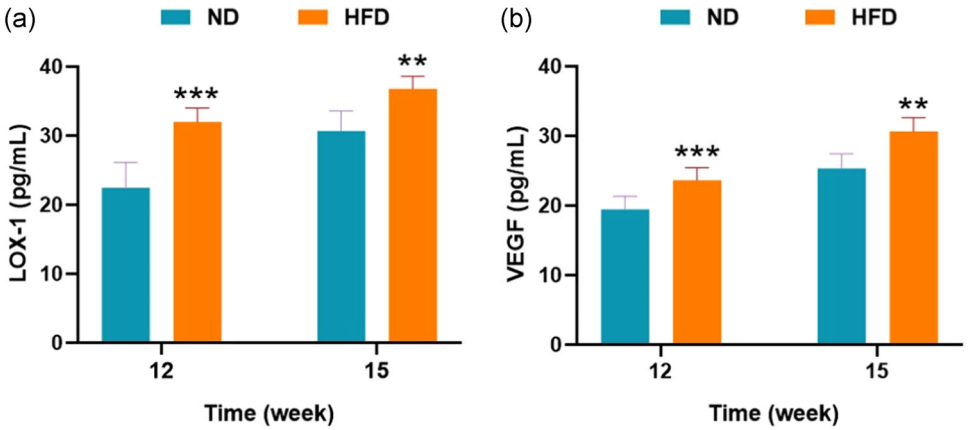

FIGURE 3 Evaluation of serum LOX-1 and VEGF expression at Weeks 12 and 15. (a) Quantification analysis of serum LOX-1 expression in mice. (b) Quantification of serum VEGF expression in mice. The data are shown as the mean ± standard deviation ($n = 6$). $^{**}p < 0.01$, $^{***}p < 0.001$ versus the ND group. HFD, high-fat diet; LOX-1, lectin-like oxidized low-density lipoprotein receptor-1; ND, normal diet.

emerged to show that the two diseases are directly associated [1, 18]. Nevertheless, the pathogenesis of the two diseases is complex, and the mechanism for their coexistence remains elusive. It is now recognized that the two diseases have shared risk factors, including advancing age, smoking, sedentary lifestyle, and obesity [7]. Obesity has been demonstrated to aggravate the progression of both cancer and atherosclerosis [8–10]. However, research on whether obesity can simultaneously promote the progression of the two diseases in the same individuals is rare.

The present study identified an impact of HFD-induced obesity on atherosclerosis and lung cancer in the same mice. Compared with ND, HFD promoted increases in weight and abdominal circumference. Mice fed with a HFD had higher TC, triglyceride, LDL-C, and HDL-C levels. Unlike TC, triglycerides, and LDL-C, HDL-C has been considered to protect against atherosclerosis and cancer [19]. However, mice fed a HFD had a higher LDL-C/HDL-C ratio, indicating that the protective effect of HDL-C may be inhibited by LDL-C.

The mice in this study underwent subcutaneous LLC cell transplantation on the first day of Week 13 and were then fed with a HFD or an ND for a further 3 weeks. The results showed that the local cancers were larger and heavier in the HFD group than in the ND group. Moreover, there were more metastatic cancers in the lung in the HFD group than in the ND group. Furthermore, the burden of aortic atherosclerosis was greater in the HFD group. Our study shows that a HFD could promote the growth and metastasis of lung cancer as well as the development of atherosclerosis in the same mice and provides direct evidence that obesity could contribute to the simultaneous progression of atherosclerosis and cancer in the same individual.

To further elucidate the underlying mechanism for obesity-induced progression of atherosclerosis and lung cancer, we investigated the change in expression of LOX-1, which is the primary receptor for ox-LDL and is responsible for the recognition, binding, and internalization of ox-LDL [20, 21]. LOX-1 is mainly expressed in endothelial cells and macrophages [14, 20]. It is well established that LOX-1 is a crucial driver of ASCVD [21, 22]. It has also been demonstrated that LOX-1 is upregulated in various types of cancer [14]. The mechanism for the involvement of LOX-1 in atherosclerosis and cancer may involve its ability to enhance proinflammatory signaling pathways and proangiogenic proteins [14].

Inflammation is widely accepted to be a prominent element during the progression of atherosclerosis and tumorigenesis [23–27]. Monocytes and macrophages are the most important cells in the innate immune system and play key roles in the pathogenesis of atherosclerosis and cancer [16, 28–31]. The quantities, polarization states, and ratios of the different types of macrophages affect the progression of both diseases [16, 30]. Tumor-associated macrophages play an important role in the development of cancer [16]. Pro-inflammatory M1 macrophages have an enhanced ability to destroy cancer cells and increase the antitumor immune response [16], whereas anti-inflammatory M2 macrophages produce low amounts of cytokines. Transforming tumor-associated macrophages by M2 polarization into the tumor-suppressive M1 phenotype is an important approach in tumor therapy [16]. LOX-1 has been shown to play a key role during M1 polarization induced by the naturally occurring mild ox-LDL found in the serum of patients with hypercholesterolemia [32].

Our present findings indicate that HFD could promote the expression of LOX-1. We also observed a change in inflammation-related immune cells, including monocytes and macrophages. The percentages of both monocytes and

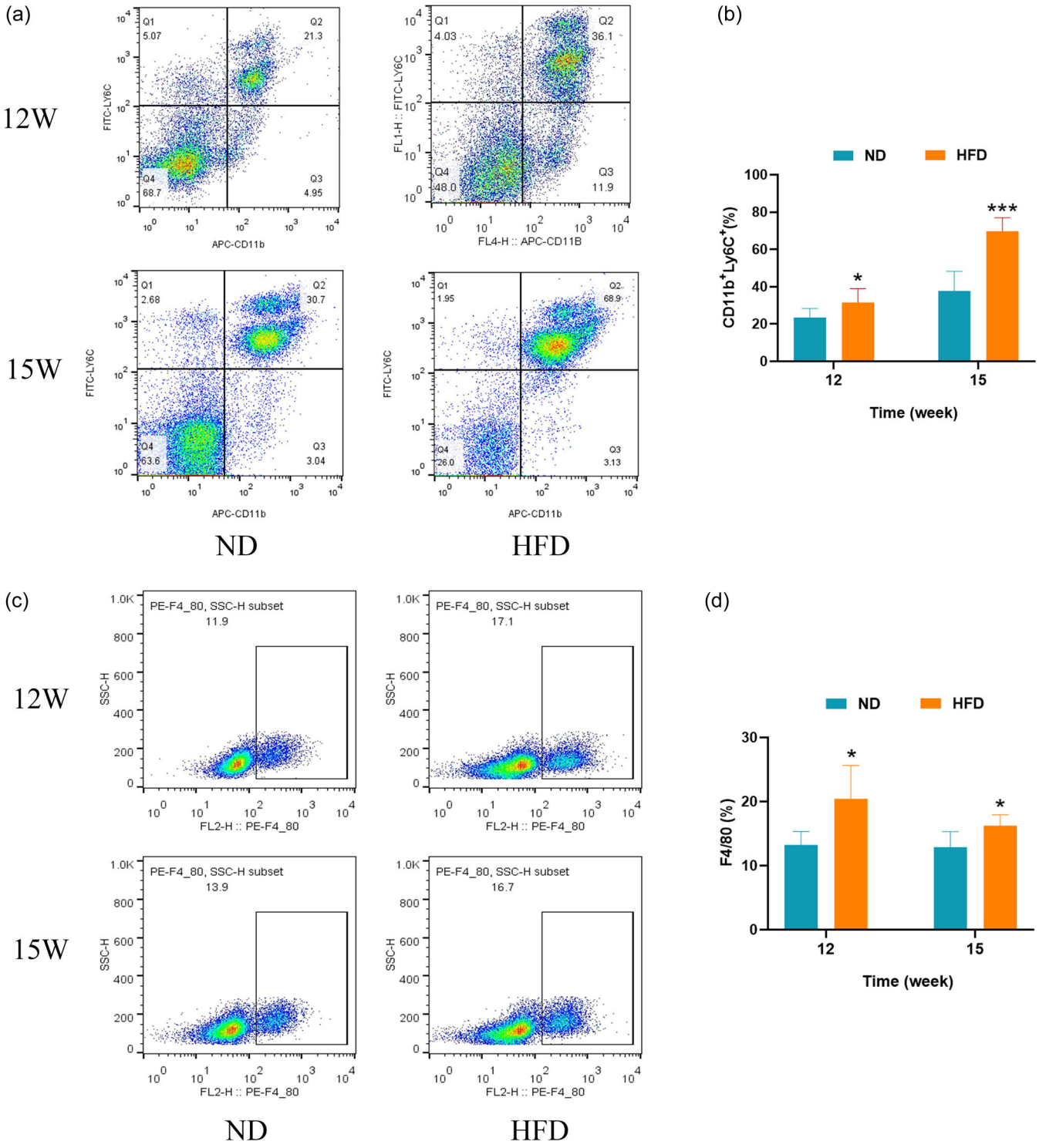

FIGURE 4 Comparison of blood monocytes and macrophages. (a) Representative flow cytometry plots of monocytes at Weeks 12 and 15 in the ND group and the HFD group. (b) Quantification analysis of monocytes in the two groups. (c) Representative flow cytometry plots of macrophages at Weeks 12 and 15 in the ND and HFD groups. (d) Quantification analysis of macrophages in the two groups. The data are shown as the mean ± standard deviation ($n = 6$). *$p < 0.05$, ***$p < 0.001$ versus the ND group. HFD, high-fat diet; ND, normal diet.

macrophages were increased in the HFD group in comparison with the ND group. Moreover, VEGF is required for tumor growth and metastasis because a blood supply is necessary for the growth and dissemination of a tumor [33]. LOX-1 activated by ox-LDL could promote upregulation of VEGF [20]. In the present study, mice in the HFD group showed a trend of increasing LOX-1, VEGF, and inflammatory cells at Weeks 12 and 15.

In view of the above findings, it is reasonable to infer that HFD-induced obesity likely promotes the simultaneous progression of lung cancer and atherosclerosis via a LOX-1-related pathway that upregulates the inflammatory response and VEGF. HFD promoted metabolic disease by increasing LDL-C, which in turn induces the expression of LOX-1. Upregulation of LOX-1 could increase the inflammatory response and serum VEGF, not only promoting atherosclerosis but also accelerating the development and metastasis of lung cancer.

There are still some limitations in the experiment. The present study indicates that obesity promotes the simultaneous progression of lung cancer and atherosclerosis in the same individual, likely through the LOX-1-related pathway. But its specific mechanism and pathway are not yet clear. In future experiments, it is recommended to include additional validation of the key genes identified to enhance the experimental findings.

5 | CONCLUSION

Based on the results of this study, it is reasonable to conclude that HFD-induced obesity can simultaneously promote the progression of lung cancer and atherosclerosis in the same individual. Our findings indicate that HFD-induced upregulation of LOX-1 may play an important role in the underlying mechanism via an inflammatory response and VEGF. However, the molecular mechanism for the effect of LOX-1 on the simultaneous progression of lung cancer and atherosclerosis needs further study.

AUTHOR CONTRIBUTIONS

Yihao Wang: Data curation (lead); methodology (equal); writing—original draft (equal). **Kaixin Yan**: Data curation (lead); methodology (lead). **Han Duan**: Data curation (supporting); methodology (supporting). **Ning Tao**: Formal analysis (equal). **Shaoning Zhu**: Data curation (supporting). **Yuning Zhang**: Methodology (supporting). **Yonggang You**: Data curation (supporting). **Zhen Zhang**: Formal analysis (supporting). **Hua Wang**: Methodology (lead); project administration (lead); writing—review and editing (supporting). **Shunying Hu**: Conceptualization (lead); funding acquisition (lead); writing—original draft (lead).

ACKNOWLEDGMENTS

We appreciate the participation of Wuhan Servicebio Technology Co., Ltd. in the preparation of pathological samples in the study.

CONFLICT OF INTEREST STATEMENT

The authors declare no conflict of interest.

DATA AVAILABILITY STATEMENT

The data that support the findings of this study are available from the corresponding author upon reasonable request.

ETHICS STATEMENT

The study was approved by the Institutional Animal Care and Use Committee at our Laboratory Animal Center (IACUC-DWZX-2020-791) and was performed in accordance with the relevant guidelines.

INFORMED CONSENT

Not applicable.

ORCID

Shunying Hu http://orcid.org/0000-0002-8738-7417

REFERENCES

1. Tapia-Vieyra JV, Delgado-Coello B, Mas-Oliva J. Atherosclerosis and cancer; A resemblance with far-reaching implications. Arch Med Res. 2017;48(1):12–26. https://doi.org/10.1016/j.arcmed.2017.03.005
2. Zigmond ZM, Song L, Martinez L, Lassance-Soares RM, Velazquez OC, Vazquez-Padron RI. C-Kit expression in smooth muscle cells reduces atherosclerosis burden in hyperlipidemic mice. Atherosclerosis. 2021;324:133–40. https://doi.org/10.1016/j.atherosclerosis.2021.03.004
3. Virani SS, Alonso A, Benjamin EJ, Bittencourt MS, Callaway CW, Carson AP, et al. Heart disease and stroke statistics-2020 update: a report from the American heart association. Circulation. 2020;141(9):e139–596. https://doi.org/10.1161/CIR.0000000000000757
4. Meltzer PS, Kallioniemi A, Trent JM. Chromosome alterations in human solid tumors. In: Vogelstein B, Kinzler KW, editors. The genetic basis of human cancer. New York: McGraw-Hill; 2002. p. 93–113.
5. Kim BJ, Kim JY, Chang DK, Son HJ, Rhee PL, Kim JJ, et al. Coexistence between carotid artery stenosis and colorectal adenomatous polyps in middle-aged men. Digestion. 2010;81(1):20–6. https://doi.org/10.1159/000217451
6. Suzuki M, Tomoike H, Sumiyoshi T, Nagatomo Y, Hosoda T, Nagayama M, et al. Incidence of cancers in patients with atherosclerotic cardiovascular diseases. IJC HeartVasc. 2017;17:11–6. https://doi.org/10.1016/j.ijcha.2017.08.004
7. Raposeiras Roubín S, Cordero A. La relación bidireccional entre el cáncer y la ateroesclerosis. Rev Esp Cardiol. 2019;72(6):487–94. https://doi.org/10.1016/j.rec.2018.12.010

8. Shi D, Wu J, Wu Y, Lin X, Xu C, Lian X. High-fat diet-related obesity promotes urethane-induced lung tumorigenesis in C57BL/6J mice. Front Oncol. 2021;11:620993. https://doi.org/10.3389/fonc.2021.620993
9. Zhang Y, Li S, Li F, Lv C, Yang Q. High-fat diet impairs ferroptosis and promotes cancer invasiveness via downregulating tumor suppressor ACSL4 in lung adenocarcinoma. Biol Direct. 2021;16(1):10. https://doi.org/10.1186/s13062-021-00294-7
10. Li S, Wu T, Lu YX, Wang JX, Yu FH, Yang MZ, et al. Obesity promotes gastric cancer metastasis via diacylglycerol acyltransferase 2-dependent lipid droplets accumulation and redox homeostasis. Redox Biol. 2020;36:101596. https://doi.org/10.1016/j.redox.2020.101596
11. Sun M, Yang Q, Li M, Jing J, Zhou H, Chen Y, et al. Associação entre a gravidade da doença arterial coronariana e câncer de pulmão: um estudo piloto transversal. Arq Bras Cardiol. 2021;118(2):478–85. https://doi.org/10.36660/abc.20200478
12. Zhao YW, Yan KX, Sun MZ, Wang YH, Chen YD, Hu SY. Inflammation-based different association between anatomical severity of coronary artery disease and lung cancer. J Geriat Cardiol. 2022;19(8):575–82. https://doi.org/10.11909/j.issn.1671-5411.2022.08.003
13. Jin P, Cong S. LOX-1 and atherosclerotic-related diseases. Clin Chim Acta. 2019;491:24–9. https://doi.org/10.1016/j.cca.2019.01.006
14. Balzan S, Lubrano V. LOX-1 receptor: a potential link in atherosclerosis and cancer. Life Sci. 2018;198:79–86. https://doi.org/10.1016/j.lfs.2018.02.024
15. Moore KJ, Tabas I. Macrophages in the pathogenesis of atherosclerosis. Cell. 2011;145(3):341–55. https://doi.org/10.1016/j.cell.2011.04.005
16. Zhang J, Zhou X, Hao H. Macrophage phenotype-switching in cancer. Eur J Pharmacol. 2022;931:175229. https://doi.org/10.1016/j.ejphar.2022.175229
17. Rekhi UR, Catunda RQ, Alexiou M, Sharma M, Fong A, Febbraio M. Impact of a CD36 inhibitor on *Porphyromonas gingivalis* mediated atherosclerosis. Arch Oral Biol. 2021;126:105129. https://doi.org/10.1016/j.archoralbio.2021.105129
18. Battisti NML, Welch CA, Sweeting M, de Belder M, Deanfield J, Weston C, et al. Prevalence of cardiovascular disease in patients with potentially curable malignancies. JACC CardioOncol. 2022;4(2):238–53. https://doi.org/10.1016/j.jaccao.2022.03.004
19. Ossoli A, Wolska A, Remaley AT, Gomaraschi M. High-density lipoproteins: a promising tool against cancer. Biochim Biophys Acta Mol Cell Biol Lipids. 2022;1867(1):159068. https://doi.org/10.1016/j.bbalip.2021.159068
20. Murdocca M, de Masi C, Pucci S, Mango R, Novelli G, di Natale C, et al. LOX-1 and cancer: an indissoluble liaison. Cancer Gene Ther. 2021;28(10–11):1088–98. https://doi.org/10.1038/s41417-020-00279-0
21. Ding Z, Pothineni NVK, Goel A, Lüscher TF, Mehta JL. PCSK9 and inflammation: role of shear stress, pro-inflammatory cytokines, and LOX-1. Cardiovasc Res. 2020;116(5):908–15. https://doi.org/10.1093/cvr/cvz313
22. Akhmedov A, Sawamura T, Chen CH, Kraler S, Vdovenko D, Lüscher TF. Lectin-like oxidized low-density lipoprotein receptor-1 (LOX-1): a crucial driver of atherosclerotic cardiovascular disease. Eur Heart J. 2021;42(18):1797–807. https://doi.org/10.1093/eurheartj/ehaa770
23. Libby P. Inflammation in atherosclerosis. Nature. 2002;420:868–74. https://doi.org/10.1038/nature01323
24. Libby P. Inflammation in atherosclerosis-no longer a theory. Clin Chem. 2021;67(1):131–42. https://doi.org/10.1093/clinchem/hvaa275
25. Khansari N, Shakiba Y, Mahmoudi M. Chronic inflammation and oxidative stress as a major cause of age-related diseases and cancer. Recent Patent Inflam Allergy Drug Discov. 2009;3(1):73–80. https://doi.org/10.2174/187221309787158371
26. Cho WC, Kwan CK, Yau S, So PP, Poon PC, Au JS. The role of inflammation in the pathogenesis of lung cancer. Expert Opin Ther Targets. 2011;15(9):1127–37. https://doi.org/10.1517/14728222.2011.599801
27. O'Byrne KJ, Dalgleish AG. Chronic immune activation and inflammation as the cause of malignancy. Br J Cancer. 2001;85(4):473–83. https://doi.org/10.1054/bjoc.2001.1943
28. Shi W, Huang Y, Yang Z, Zhu L, Yu B. Reduction of TMAO level enhances the stability of carotid atherosclerotic plaque through promoting macrophage M2 polarization and efferocytosis. Biosci Rep. 2021;41(6):BSR20204250. https://doi.org/10.1042/BSR20204250
29. Yadav S, Dwivedi A, Tripathi A. Biology of macrophage fate decision: implication in inflammatory disorders. Cell Biol Int. 2022;46(10):1539–56. https://doi.org/10.1002/cbin.11854
30. Eshghjoo S, Kim DM, Jayaraman A, Sun Y, Alaniz RC. Macrophage polarization in atherosclerosis. Genes. 2022;13(5):756. https://doi.org/10.3390/genes13050756
31. Lee-Rueckert M, Lappalainen J, Kovanen PT, Escola-Gil JC. Lipid-laden macrophages and inflammation in atherosclerosis and cancer: an integrative view. Front Cardiovasc Med. 2022;9:777822. https://doi.org/10.3389/fcvm.2022.777822
32. Chang SF, Chang PY, Chou YC, Lu SC. Electronegative LDL induces M1 polarization of human macrophages through a LOX-1-dependent pathway. Inflammation. 2020;43(4):1524–35. https://doi.org/10.1007/s10753-020-01229-6
33. Kapoor P, Deshmukh R. VEGF: a critical driver for angiogenesis and subsequent tumor growth: an IHC study. J Oral Maxillofac Pathol. 2012;16(3):330–7. https://doi.org/10.4103/0973-029X.102478

SUPPORTING INFORMATION

Additional supporting information can be found online in the Supporting Information section at the end of this article.

How to cite this article: Wang Y, Yan K, Duan H, Tao N, Zhu S, Zhang Y, et al. High-fat-diet-induced obesity promotes simultaneous progression of lung cancer and atherosclerosis in apolipoprotein E-knockout mice. Cancer Innov. 2024;3:e127. https://doi.org/10.1002/cai2.127